

# Articles

## Electrochemical Studies on the Mechanism of the Fabrication of Ceramic Films by Hydrothermal-Electrochemical Technique<sup>†</sup>

Zhibin Wu and Masahiro Yoshimura\*

Center for Materials Design, Materials and Structures Laboratory, Tokyo Institute of Technology, Yokohama 228-8503, Japan

Received March 6, 1999

In this paper, electrochemical techniques are used to investigate hydrothermal-electrochemically formation of barium titanate (BT) ceramic films. For comparison, the electrochemical behaviors of anodic titanium oxide films formed in alkaline solution were also investigated both at room temperature and in hydrothermal condition at 150 °C. Film structure and morphology were identified by scanning electron microscopy (SEM) and atomic force microscopy (AFM). Titanium oxide films produced at different potentials exhibit different film morphology. The breakdown of titanium oxide films anodic growth on Ti electrode plays an important role in the formation of BT films. BT films can grow on anodic oxide/metal substrate interface by short-circuit path, and the dissolution-precipitation processes on the ceramic film/solution interface control the film structure and morphology. Based upon the current experimental results and our previous work, extensively schematic procedures are proposed to model the mechanism of ceramic film formation by hydrothermal-electrochemical method.

### Introduction

In recent years, our group has pioneered the development of a new technique that uses hydrothermal-electrochemical method to in situ fabricate morphology-controlled crystalline ceramic thin films.<sup>1,2</sup> This technique, which belongs to so-called soft solution processing (SSP), concerns the fabrication, shaping, sizing and orientation of ceramics in aqueous solution in one step without excess energies for firing, sintering or melting. It offers the advantage of enhanced purity, lower reaction temperature and higher film growth rate.

Hydrothermal-electrochemical method has been proven to be a powerful technique to fabricate ceramic thin films.<sup>1-3</sup> It is well accepted that the formation of ceramic films by hydrothermal-electrochemical method generally follows the dissolution-crystallization mechanism,<sup>1</sup> but the detailed procedures have been a puzzle to scientists engaged in the area. How does the film formation start? How does the film grow? Can the film grow infinitely? And why does electrochemical reaction accelerate hydrothermal formation of ceramic films? Several efforts to understand the process have been made. Vargas *et al.*<sup>3</sup> electrochemically characterized the hydrothermal-electrochemical formation of BaTiO<sub>3</sub> films at the early stages of growth under potentiostatic conditions and concluded that hydrothermal-electrochemical BaTiO<sub>3</sub> film formation is initially controlled by charge transfer related to the electrochemical oxidation of titanium. The later process becomes a mass transfer controlled process corresponding to the diffusion of Ba<sup>2+</sup> ions across the built-up BaTiO<sub>3</sub> layer. Bacsá *et al.*<sup>4</sup> suggested that after the first layer

of BaTiO<sub>3</sub> is formed the growth continues, possibly because of the dissolution of BaTiO<sub>3</sub> during the process. The dissolution of BaTiO<sub>3</sub> may expose fresh metal surface to the electrolyte and the reaction may continue through the pores formed. Bendale *et al.*<sup>6</sup> proposed a model to interpret the film formation and growth mechanism, which contains three steps: (1) formation of either a Ti oxide or hydrous oxide film, (2) nucleation of fine BaTiO<sub>3</sub> crystallites on the surface of the Ti oxide film and growth to form insulating polycrystalline BaTiO<sub>3</sub> film, and (3) the dielectric breakdown of the films if the cell voltage exceeds a critical values. According to the model, the film grows at the film surface by the cyclic process consisting of the deposition of BaTiO<sub>3</sub> crystallites and the transport of Ti-bearing species from the Ti oxide film to the film surface through fissures and holes created by the breakdown. As a result, the film growth interface is in the solution/film interface. A series of studies have been done by Kajiyoshi and Yoshimura on the growth mechanism of ATiO<sub>3</sub> (A = Ba, Sr) film by the hydrothermal-electrochemical method.<sup>8-13</sup> A short-circuit diffusion model was proposed to determine the film growth mechanism by the hydrothermal-electrochemical method.<sup>11</sup> The very important point concerning the growth of film in the model is the concept of short-circuit paths. It is supposed that A-site and O atoms diffuse as solution species through open pores that are extending as microcapillaries from the film surface to the Ti electrode. The conclusion is that the ATiO<sub>3</sub> films grows mainly at the film/electrode interface. Successively, during the film growth, A-site and O atoms preexisting in ATiO<sub>3</sub> grains are mixed with respective atoms in the solution by an atom-mixing mechanism accompanying a dissolution-recrystallization, which proceeds on grain surfaces in contact with the solution.<sup>8</sup> However, all available works concerning studies of the mechanism stress only certain parts.

The phenomenon of breakdown in growing anodic oxides

\*To whom correspondence should be addressed. Tel: +81-45-924-5323. Fax: +81-45-924-5358. E-mail: Yoshimu1@rlem.titech.ac.jp

<sup>†</sup>Basis of the presentation given at International Joint Seminar on New Trends in Material Chemistry 12-13 March 1999, Seoul National University, Seoul, Korea

films has led to much research into understanding the growth mechanism of anodic oxides films and structural changes in the oxides film.<sup>14-18</sup> An extensive illustration of the processes involved in anodic oxide growth and breakdown is given in ref. 14. Generally speaking, the elementary processes involved in anodic oxide growth and breakdown mainly include the electrons and ionic species migration to oxide/electrolyte surface and injection into the oxide from the outer oxide boundary, and the generation of oxygen anions presumably by water decomposition. We thought that the breakdown of anodic oxides film should play an important role in the fabrication of ceramic films by hydrothermal-electrochemical method. In this study, the mechanism of the synthesis of ceramic films by hydrothermal-electrochemical method was addressed through the electrochemical investigations on the formation and breakdown of anodic oxide and the roles in the formation of ceramic films. Hydrothermal-electrochemically formed barium titanate (BT) ceramic films were used as model compounds. Except for the electrochemical technique, the characterization of films fabricated in different conditions was also carried out by scanning electron microscopy (SEM) and atomic force microscopy (AFM), which is considered a useful tool that allows not only direct surface observation with three-dimensional imaging at nanometric resolution, but also quantification of the surface roughness. As a result, an extensive schematical procedure was developed to interpret the whole process of the fabrication of ceramic films by hydrothermal-electrochemical method.

### Experimental Section

Titanium metal substrate with 99.9% purity and measuring 5 mm × 40 mm × 0.5 mm were used as working anodic electrode to fabricate barium titanate films. Metal substrates were mechanically polished to a mirror finish. Before anodic deposition, titanium or tantalate plates were degreased in hot acetone with an ultrasonic cleaner, etched in a chromic acid mixture for about 16 hours, and then washed in distilled water with the ultrasonic cleaner. Ba(OH)<sub>2</sub> and KOH solution was prepared: Ba(OH)<sub>2</sub> · 8H<sub>2</sub>O and KOH (guaranteed reagent) with boiling distilled water in order to remove dissolved CO<sub>2</sub> that could produce insoluble carbonates.

To fabricate barium titanate by the hydrothermal-electrochemical method, Teflon beaker containing the electrolyte was placed in a cell of an autoclave equipped with a three electrode system. Ti and Pt plates served as the working electrode and counter electrode, respectively. An Ag/AgCl external electrode (Toshin Kogyo, Tokyo, Japan) was used as the reference electrode. All experiments were performed under galvanostatic conditions with the current density varying from 0.5 mA/cm<sup>2</sup> to 10 mA/cm<sup>2</sup> provided by a potentiostat (potentiostat/Galvanostat 2000, Toho Technical Research) in 0.25 M Ba(OH)<sub>2</sub> for BT. Changes in potential as a function of reaction time were recorded by personal computer for selected experiments. The temperature for hydrothermal-electrochemical treatment was controlled at 150 °C, and the reaction cell was kept at the saturated vapor pressure

at this temperature. After each experiment, the Ti substrates with BT film were washed by water, ultrasonicated in ethanol, and air-dried before characterization. Samples were stored in covered containers in a desiccant.

A titanium disk electrode was used as a working electrode to run the impedance experiments at room temperature. The disk working electrode, 0.5 cm in diameter, was constructed from titanium rod (99.95%) embedded in a shrinkable PTEF tube. The reference electrode was a saturated calomel electrode (SCE). All the potentials were referred to this reference electrode. A platinum flag served as a counter electrode. The electrolyte used in all the experiments was a 1.0 M KOH solution freshly prepared with reagent grade potassium hydroxide and boiled distilled water. The freshly polished titanium electrode was first conditioned with the electrode potential at -1.6 V for 10 min in 1.0 M KOH solution. After which the titanium electrode was kept at a chosen potential for 1 hour to produce oxides film before running electrochemical impedance spectroscopy (EIS) experiments.

The EIS for titanium oxide film samples was carried out by an EG&G PAR Model 273A potentiostat equipped with an EG&G model 5210 lock-in amplifier at formation potentials for samples under argon atmosphere. The instrument was controlled by EG&G 398 software through a personal computer. The imposed ac signal was 5 mV rms. In the high frequency region of 10<sup>5</sup>~5 Hz, a single sine model was fixed, and in the low frequency region, the measurement was made at multisine mode. A constant phase element (CPE) was used for data fitting instead of an ideal capacitor. The spectra were analyzed using the nonlinear least software program, Equivalent Circuit provided by Universiteit Twente through EG&G company.

The surface morphology of the grown film was investigated both by scanning electron microscopy (SEM) (SEM, Model S-4000, Hitachi, Tokyo, Japan) and by atomic force microscopy (AFM) (Digital Instruments Nanoscope III, USA) operating in the contact mode. AFM images were taken at a resolution of 512 × 512 pixels without low-pass filtering. Silicon nitride cantilevers with a spring constant of 0.38 N/m were used for all images.

### Results and Discussion

#### Dissolution and precipitation behaviors of Ti oxide film in alkaline solution

**The EIS spectra.** The electrochemical impedance spectra of titanium oxide films formed in different potentials were recorded for the films prepared between -0.4 V and 1.0 V. When the films were formed below the potential of 0.6 V, the spectra showed a diffusion tail at the low frequency. Typical figures for the films formed at -0.4 V are shown in Figure 1A. An insert in Figure 1A shows an equivalent circuit to best fit the data shown in Figure 1A. The simulated values for elements based on the equivalent circuits are shown in Figures 1A and 1B. The R<sub>s</sub> component in the circuit is the solution resistance. The n value of CPE Q1 is close to 1.0, indicating that this is a double-layer capacitor. A Warburg

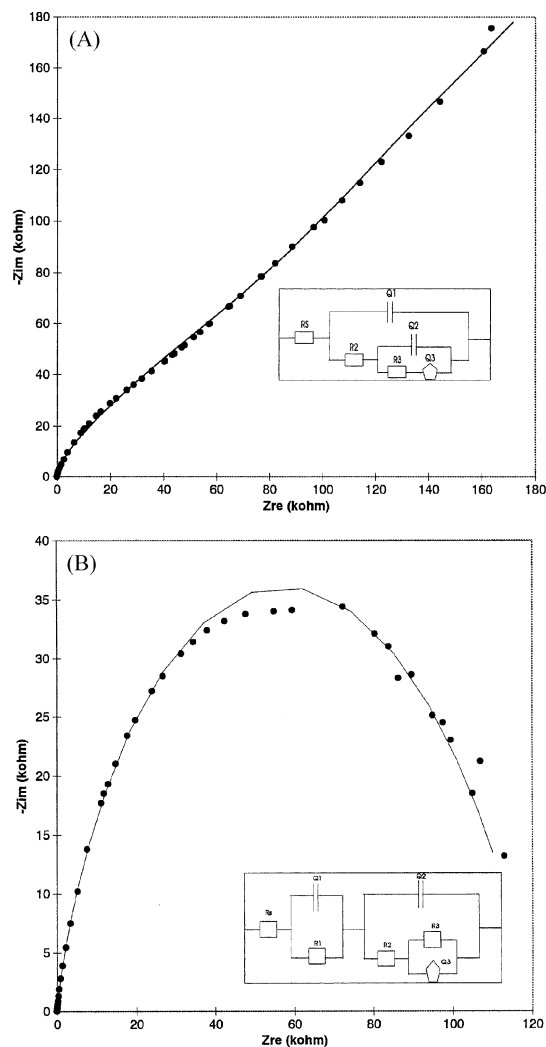


**Figure 1.** Complex impedance spectra for a titanium disk electrode in 1.0 M KOH at the potential of (A) -0.4 V, (B) 0.6 V, respectively. Dotted points are experimental data, solid line are simulations according to the equivalent circuits of the insets. For Figure 1A,  $R_s = 7.5 \Omega$ ;  $R_2 = 225 \Omega$ ;  $R_3 = 89.4 \text{ k}\Omega$ ;  $Y_{Q1} = 4.24 \times 10^{-6}$ ,  $n = 0.95$ ;  $Y_{Q2} = 18.3 \times 10^{-6}$ ,  $n = 0.82$ ;  $Y_{Q3} = 15.7 \times 10^{-6}$ ,  $n = 0.55$ . For Figure 1B,  $R_s = 9.5 \Omega$ ;  $R_1 = 33.8 \Omega$ ;  $R_2 = 1.52 \text{ k}\Omega$ ;  $R_3 = 120 \Omega$ ;  $Y_{Q1} = 4.92 \times 10^{-6}$ ,  $n = 0.98$ ;  $Y_{Q2} = 2.66 \times 10^{-6}$ ,  $n = 0.98$ ;  $Y_{Q3} = 8.92 \times 10^{-6}$ ,  $n = 0.61$ .

component of CPE Q3 with an  $n$  value close to 0.5 was observed, which indicates that the diffusion of the oxidation products resulting in the dissolution of oxide films exist in this system. The CPE Q2 with the  $n$  values of about 0.8 shows an intermediate character between a capacitor ( $n = 1$ ) and a Warburg impedance ( $n = 0.5$ ). Q2 may be related to the adsorbed intermediate species generated during the dissolution process and subsequently adsorbed on the electrode surface. These adsorbed intermediate species may hinder the diffusion process due to oxidation. Therefore, these adsorbed intermediate species are believed to be the reason for the repassivation. The approximated semicircles impedance spectra were recorded with a potential higher than 0.6 V (Figure 1B). The best equivalent circuit for fitting the data is shown in the insert of Figure 1B. Two continuous semicircles were found in the equivalent circuits. The semicircle at high

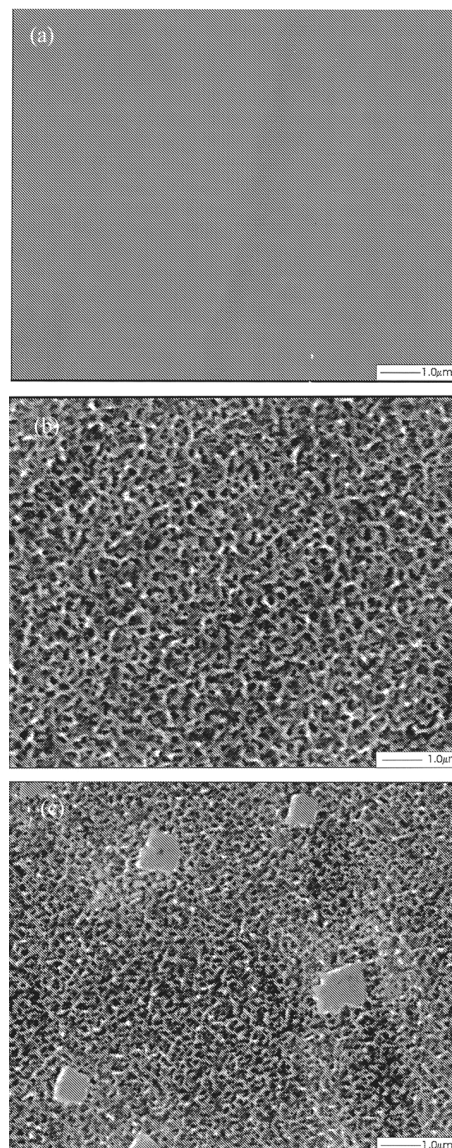


**Figure 2.** SEM micrography of titanium oxide anodic films formed at different potentials in 1.0 M KOH: (A) -0.4V, (B) 0.4 V, and (C) 8.0V.

frequencies (the R1-Q1 parallel network shown in the left of Figure 4B) is attributed to the faradaic charge transfer process, while the second circle is attributed to an adsorbed species that contributes to the repassivation.

The SEM image of the film formed at potential -0.4 V shows a homogeneous structure without cracks and micro-porous at the micrometer scale (Figure 2A). The image of the films formed at the potential larger than 0.0 V show an amorphous porous structure (Figure 2B). As shown in Figure 2C, the SEM image of the films formed at potential larger than 8.0 V, crystallites can be observed on the amorphous film surface.

**The growth of titanium oxide films under hydrothermal-electrochemical conditions.** Under hydrothermal-electrochemical conditions at 150 °C, titanium oxide film were grown by a constant current flowing through the titanium anode electrode. The increasing oxide thickness cause an increased voltage drop in the oxide. As the anodic potential increased to a certain value, the breakdown potential ( $V_b$ ), the anodic oxide

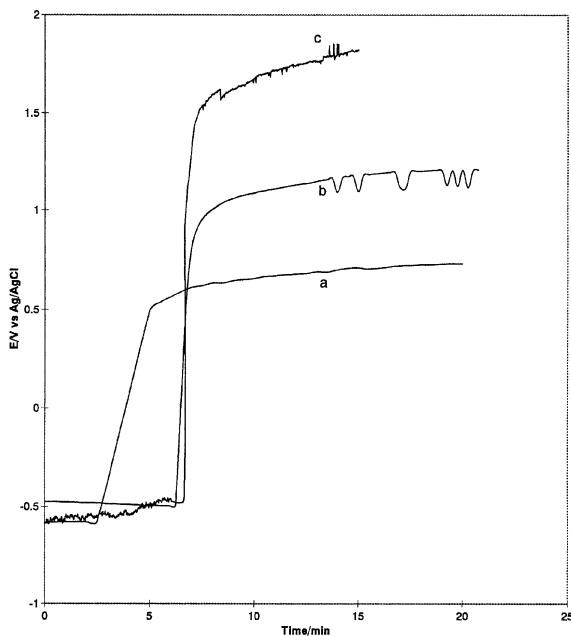


**Figure 3.** Cell voltage as a function of time for samples prepared at current density of a: 0.5, b: 5.0, and c: 10 mA/cm<sup>2</sup>, respectively. Ti electrode, 0.5 M KOH, 150 °C.

film would breakdown, resulting in the dissolution of titanium oxide. Typical anodic growth kinetic curves are shown in Figure 3, which display the kinetic behavior of the anodization of titanium electrode in 0.5 M KOH solution in a range of current densities between 0.5 mA/cm<sup>2</sup> to 10 mA/cm<sup>2</sup>.

The slopes of the potential increase as the current densities, indicating that the rate of increasing potential is much faster at the high current density than the lower one. It can be inferred that the oxidation of Ti and the film growth are related to the current density. On the other hand, it is believed that the voltage oscillation as a function of time are the result of breakdown caused by simultaneous oxide growth and dissolution processes.<sup>14</sup> Such kinetics indicate that under hydrothermal conditions, the titanium oxide can be electrically broken down, with dissolution occurring simultaneously with oxide growth in alkaline solution at a faster rate. Electron scanning microscopy experiments are consistent with kinetic growth curves. Very small fissures and porous film structure were discovered (Figure 4).

**Dissolution and precipitation behaviors of Ti oxide film in alkaline solution.** The mechanism of anodic titanium oxide film dissolution is not well understood in alkaline solutions, accounting for the extensive illustration of the processes of anodic oxide growth and breakdown.<sup>14</sup> In this system, it is thought that the electrons and electrolyte injection into anodes film and the oxygen evolution caused the film electric breakdown. The higher tendency for titanium oxide film to react with hydroxyl group to form hydrous oxides and dissolve in alkaline titanium could be another reason, according to the Pourbaix diagram.<sup>19</sup> Moreover, hydroxyl groups in alkaline electrolytes could adsorb at the surface of the growing oxide through diffusion and further incorporated into the oxide bulk. They may play an impor-

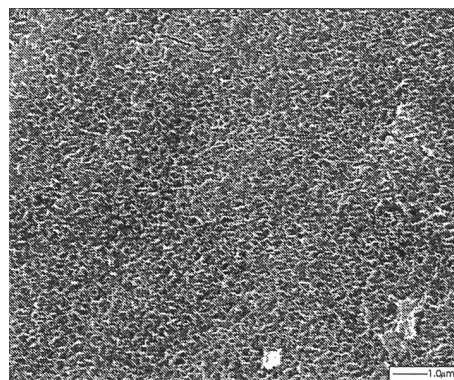


**Figure 4.** SEM image of anodic titanium oxide films grown in 0.5 M KOH at 150°C under  $i=5$  mA/cm<sup>2</sup>.

tant role in the dissolution of the oxide films. Obviously, the fissure structure and porous morphology shown in Figure 2 and Figure 4 result in the breakdown and dissolution of oxide film reacted with the hydroxyl groups in alkaline solution.

EIS experimental results show that the dissolved hydroxyl titanium oxide could precipitate again along with the dissolution of titanium oxide, which corresponds with the anodic overpotential. At the low anodic overpotential, both the dissolution and precipitation processes are slow, as a result homogeneous morphology of the oxide films (Figure 2A) was observed. Additional positive overpotentials result not only in increasing the dissolution of the titanium oxide film, but also in increasing the concentration of dissolved titanate (probably is  $\text{HTiO}_3^-$ <sup>19</sup>) and the precipitation rate. The titanium hydroxyl ions existing in solution become anhydrous oxides again and deposit on the porous oxide film surface (Figure 2C).

#### The growth of barium titanate films at titanium electrode under hydrothermal-electrochemical condition

**The kinetic behaviors.** Typical anodic potentials versus time curves under different current densities for the kinetics of BT films are shown in Figure 5. The anodic voltage increased to the breakdown potential, then reach a certain stationary value when current was passed through the Ti anodic electrode in 0.25 M  $\text{Ba}(\text{OH})_2$  solution under hydrothermal condition at 150 °C. In curve b, a shoulder peak was observed at about 2V. After the shoulder, the potential still increased with the current injection, and the slope of the growth curve is almost the same as the slope before the shoulder potential. It is observed that the shoulder potential is random and sometime missing. The observed breakdown voltage is about 10 V. The breakdown strength for polycrystalline barium titanate is approximately  $1.2 \times 10^5$  V/cm.<sup>20</sup> It could be estimated that the breakdown voltage is about 12V for the film with a thickness of 1  $\mu\text{m}$ , which is similar to the observed values.

It could be supposed that the BT film formation originating from the Ti oxide film breakdown grows on the Ti anode surface as the potential increased. After the Ti oxide dissolved to form  $\text{HTiO}_3^-$  ion, the supersaturation of barium titanate is quickly met, precipitating on the Ti oxide surface, which causes the new potential drop on the Ti surface. The

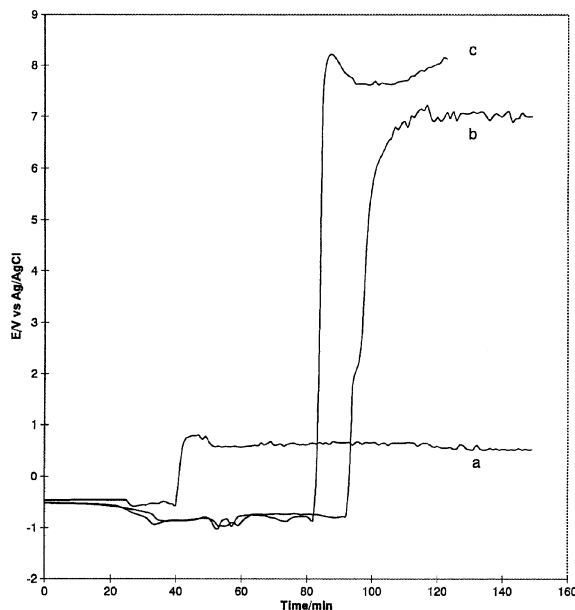


**Figure 5.** Cell voltage as a function of time for samples prepared at current density of a: 0.5, b: 5.0, and c: 10 mA/cm<sup>2</sup>, respectively. Ti electrode, 0.25M Ba(OH)<sub>2</sub> (pH 14), 150 °C.

higher potential increasing slope in this range indicate that the initial formation of BT films is very fast.

The shoulder appearing in the kinetic curves could give us important information concerning the mechanism of film formation. According to the Pourbaix diagram,<sup>19</sup> once the titanium anodic is oxidized in alkaline solution, different species of titanate could be formed, such as TiO, Ti<sub>2</sub>O<sub>3</sub> and TiO<sub>2</sub>. In view of thermodynamic consideration, the reaction of TiO and Ti<sub>2</sub>O<sub>3</sub> with hydroxyl species to dissolve is much easier than for the TiO<sub>2</sub>. Therefore, the shoulder appearing in the kinetic curves infers the formation and dissolution of different titanate species. This maybe the main reason why the synthesis of ceramic films by hydrothermal-electrochemical method is rather fast and efficient compared with the hydrothermal method.

No significant changes in the slope of increasing potential among the current densities were observed, which indicated that the film growth was related only to the rate of the precipitation of the supersaturating barium titanate. Voltage oscillation as a function of time was also observed after the curves reach the breakdown potentials. This indicated that hydrothermal-electrochemically formed BT films can be broken down with increasing voltage and dissolved in solution. The dissolved BT particles could be deposited again from solution simultaneously with BT dissolution, causing the voltage oscillation. This is evidence of the well known dissolution-recrystallization mechanism.

**Characterization of BT films by AFM.** AFM surface topographies of the BT films grown on the Ti substrate are shown in Figure 6. The surface of these films is well compacted with well defined BT grains. Actually, the grain size is not uniform. It was found that there is no significant difference in the average grain size of the films prepared with different current densities in the range from 0.5 mA/cm<sup>2</sup> to

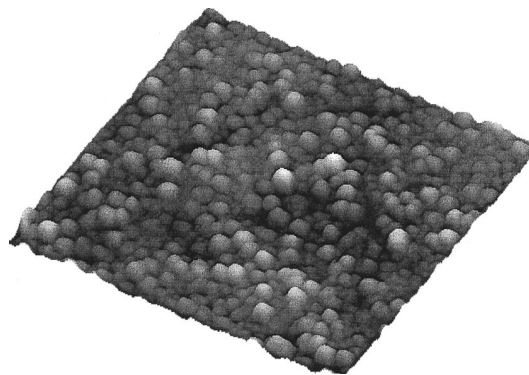


**Figure 6.** AFM image of BT film. sample prepared at Ti electrode in 0.25M Ba(OH)<sub>2</sub>(pH 14) electrolyte to react 60 min at the current density of 1 mA/cm<sup>2</sup>. Scan area of image is 10×10 μm<sup>2</sup> with a Z scale of 2.0 μm.

10 mA/cm<sup>2</sup>.<sup>21</sup> This indicates that the grain size of the BT films depends on the nucleation of fine BaTiO<sub>3</sub> crystallites on BT film/solution surface by the dissolution - recrystallization procedure. Figure 6 also shows that the upper grains are bigger than the lower ones. The larger grains are located on the outer surface, while the smaller ones are restrained by the bigger ones. This type of microstructure may indicate the grain growth mechanism is controlled by nucleation and growth process, because the largest grains are the ones that nucleated first and thus have enough time to grow. The fine grains observed in the inner place of film also indicated that the film is grown from outside the surface to inside. On the other hand, cracks and fissures appearing in the branches across the surface have been observed, which indicate the films breakdown.

**Model of the barium titanate film formation mechanisms by hydrothermal-electrochemical method.** Because of the complexity of this system, it would be difficult to describe the whole processes quantitatively. Based on the above discussion and our experimental results, the mechanism could be schematically expressed as shown in Figure 7, which shows several successive steps: (1) the anodic formation of Ti oxide films and film breakdown and dissolution, (2) the initial formation of BT supersaturating precipitates and the heterogeneous nucleation of BT crystals on the substrate surface until it covers all substrate surface, (3) the growth of BT film, and (4) the blocking of the growth of BT film.

First, Ti oxide films were formed quickly by providing either a constant voltage or current under hydrothermal-electrochemical condition. Under galvanostatic condition, the growth of Ti oxide film results in an increased voltage drop in the system. As the voltages came to breakdown potential, the Ti oxide films would breakdown, and dissolve in concentrated alkaline solution to form Ti beard hydroxyl species (probably is HTiO<sub>3</sub><sup>-</sup>). It is believed that the highly concentrated alkaline media accelerates the dissolution of Ti oxide. Simultaneously, the dissolved HTiO<sub>3</sub><sup>-</sup> ions reacted with the Ba<sup>2+</sup>, forming the supersaturating particles precipitating on the Ti oxide surface. The heterogeneous nucleation of BT crystals from solution continues until the surface is fully covered with BT grains. As a result, the dissolution of Ti-oxide

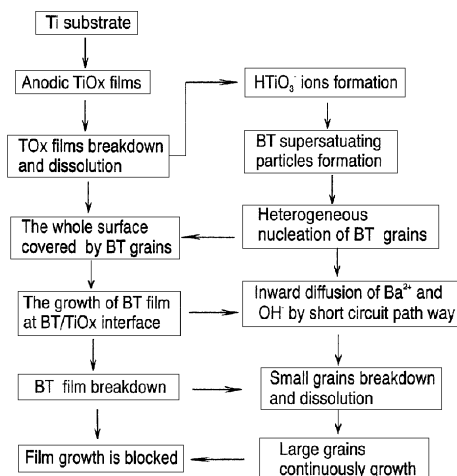


**Figure 7.** Block expression of the BT formation mechanism under hydrothermal-electrochemical method. See text for details.

is blocked somewhat. It is suggested that in this step the rate-determining reactions are the formation of Ti-oxide films and the growth of BT grains. The oxide dissolution and the precipitation of BT are very fast because of the acceleration both by electric field and high hydroxyl concentration as well as free space to deposit the supersaturating BT particles. After the entire surface is covered with BT grains, the processes are supposed to proceed to the steps of the growth of the BT film. Because the Ti-oxide has already been blocked by the freshly formed BT grains, the breakdown in the system could be attributed to the BT film breakdown resulting in the dissolution of small BT grains. This favors the growth of the crystallites in the out surface (Figure 6). The successively formed supersaturating BT particles are thought to prefer to nucleate at the formed BT grain boundaries to provide a pathway or so-called short-circuit path for the inward diffusion of  $\text{Ba}^{2+}$  and  $\text{OH}^-$  to the BT/Ti-oxide surface. This inward diffusion is much faster than the one from the bulk crystals of BT. This diffusion supplies rich  $\text{Ba}^{2+}$  and  $\text{OH}^-$  ions to BT/Ti-oxide interface to produce amorphous BT film at this interface and make the film thicker. In this stage, the BT films continue growing on both Ti-oxide/BT film interface and BT film/solution interface. However, the growth rate is gradually hindered along the thicker part of the BT film because the short-circuit paths become too narrow to transport  $\text{Ba}^{2+}$  and  $\text{OH}^-$  ions, especially when the film is densely packed. The schematic model presented here could include all the previous mechanisms proposed for this system.

### Conclusions

Based upon the experimental results outlined here for the Ti/TiOx/electrolyte system, can be concluded that:

(1) Titanium oxide films produced in different potentials or in current density exhibit different film morphology. Dissolution and precipitation behaviors of Ti oxide film in alkaline solution have been identified.

(2) The breakdown of titanium oxide films anodic growth on Ti electrode play important roles in the formation of BT films.

(3) The BT film can be formed both at Ti oxide/BT film surface and in BT/electrolyte solution. BT films grow on anodic oxide/metal substrate interface by short-circuit pathways, and the dissolution-precipitation processes on the ceramic film/solution interface, which control the film structure and morphology.

(4) The multilayer structures of BT film fabricated by hydrothermal-electrochemical technique results from the competition reaction between the rate of the growth of anodic Ti oxide films and the rate of precipitation from superconcentrating BT particles.

**Acknowledgment.** This work was supported by the Japanese Society for the Promotion of Science (JSPS) as part of the "Research for the Future Program" No. 96R06901. The authors would like to thank S. W. Song, T. Watanabe and K. Sakai for experimental assistance, and K. S. Han for valuable advice.

### References

1. Yoshimura, M. *J. Mater. Res.* **1998**, *13*, 796, and references therein.
2. Yoshimura, M.; Suchanek, W. *Solid State Ionics* **1997**, *98*, 197, and references therein.
3. Vargas, T.; Diaz, H.; Silva, C. I.; Fuenzalida, V. M. *J. Am. Ceram. Soc.* **1997**, *80*, 213.
4. Bacsa, R. R.; Rutsch, G.; Dougherty, J. P. *J. Mater. Res.* **1996**, *11*, 194.
5. Bacsa, R. R.; Ravindranathan, P.; Dougherty, J. P. *J. Mater. Res.* **1992**, *7*, 423.
6. Venigalla, S.; Bendale, P.; Ambrose, J. R.; Verink Jr., E. D.; Adair, J. H. *Mat. Res. Soc. Symp. Proc.* **1992**, *243*, 309.
7. Bendale, P.; Vengala, S.; Ambrose, J. R.; Verink, Jr., E. D.; Adair, J. H. *J. Am. Ceram. Soc.* **1993**, *76*, 2619.
8. Kajiyoshi, K.; Yoshimura, M. *Eur. J. Solid State Inorg. Chem.* **1996**, *33*, 623.
9. Kajiyoshi, K.; Hamaji, Y.; Tomono, K.; Kasanami, T.; Yoshimura, M. *J. Am. Ceram. Soc.* **1996**, *79*, 613.
10. Kajiyoshi, K.; Yoshimura, M.; Hamaji, Y.; Tomono, K.; Kasanami, T. *J. Mater. Res.* **1996**, *11*, 169.
11. Kajiyoshi, K.; Tomono, K.; Hamaji, Y.; Kasanami, T.; Yoshimura, M. *J. Am. Ceram. Soc.* **1995**, *78*, 1521.
12. Kajiyoshi, K.; Tomono, K.; Hamaji, Y.; Kasanami, T.; Yoshimura, M. *J. Am. Ceram. Soc.* **1994**, *77*, 2889.
13. Kajiyoshi, K.; Tomono, K.; Hamaji, Y.; Kasanami, T.; Yoshimura, M. *J. Mater. Res.* **1994**, *9*, 2109.
14. Parkhutik, V. P.; Albella, J. M.; Martinez-Duart, J. M. In *Modern Aspects of Electrochemistry*, Conway B. E., et al., Ed.; Peenum Press: New York, **1992**, *23*, 315.
15. DiQuarto, F.; Piazza, S.; Sunseri, C. *J. Electrochem. Soc.* **1984**, *131*, 2901.
16. Archibald, L. C.; Leach, J. S. L. *Electrochim. Acta* **1977**, *22*, 15.
17. Yahalom, J.; Zahavi, J. *Electrochim. Acta* **1970**, *15*, 1429.
18. Ikonopisov, S. *Electrochim. Acta* **1977**, *22*, 1077.
19. Pourbaix, M. In *Atlas of Electrochemical Equilibria in Aqueous Solutions*, 2nd ed., National Association of corrosion/engineers: Houston, TX, **1974**, 213.
20. Walther, G. C.; Hench, L. L. In *Physics of Electronic Ceramics*, Nair, K. M., Ed.; American Ceramic Society: Columbus, OH, **1984**; Part A, p 539.
21. Wu, Z.; Yoshimura, M. *Solid State Ionics* accepted.